American Journal of Renewable and Sustainable Energy
Vol. 4, No. 1, 2018, pp. 8-23
http://www.aiscience.org/journal/ajrse
ISSN: 2381-7437 (Print); ISSN: 2381-7445 (Online)

Investigation of a Solar Thermal Power Generation and Desalination System: An Analytical Study

Masoud Arabbeiki[1, *], Mojtaba Bakhshi[2]

[1]Department of Mechanical Engineering, Payame Noor University, Tehran, Iran
[2]Department of Chemical Engineering, Payame Noor University, Tehran, Iran

Abstract

Applying new method for a Photovoltaic-Thermal (PV-T) panel system, analytical study was performed for electricity generation as well as desalinated water production. The PV-T panel was designed with a channel under it where seawater would be housed at a constant pressure of 20 kPa and ambient temperature of 15.8°C. The surface of the PV panel was modeled by a high absorption black chrome surface. Irradiation flux on the surface and the heat addition on the saltwater was calculated hourly between 9:00 am and 6:00 pm. The desorbed air then passed through a turbine where it generated electrical power, subsequently condensing into the desalinated water at the outlet. This gave an energy generation range for the turbine of 0.24 W to 1.12 W, while the desalinated water production range was 12.35 kg/ hr.m^2 to 52 kg/ hr.m^2. System efficiency was found to be between 7.5% and 24.3% and also the desalinated water production efficiency was found to be 40% to 43%.

Keywords

Desalination, Power Generation, PV-T, Solar, Energy Conversion

Received: April 6, 2018 / Accepted: May 7, 2018 / Published online: June 7, 2018

1. Introduction

Photovoltaic (PV) solar cells/panels have typical efficiencies of 30% for silicone based panels and 10% to 19% for the thin-film based panel. PV solar panels convert visible light into an electric current using what is known as the photovoltaic effect, which was first discovered by French physicist Edmund Becquerel. However, as much as 85% of this solar radiation interacted with such panels is converted to waste heat which is a waste of a usable renewable resource. Solar thermal panels are heat exchangers that take heat from the radiation flux normal to the surface that is heated and use air or liquid as the convection median to transfer heat. A combination of both PV and thermal panels would be an efficient solution to the wasted heat by PV panels. As such, Photovoltaic-Thermal (PV-T) solar panels, also known as hybrid solar panels, use a combination of a traditional photovoltaic solar panel and solar thermal panel through a variety of design in order to use the waste heat for useful work. A single system instead of two would undoubtedly be beneficial in both space saving and improve efficiencies of the system.

PV-T solar panels use what would have been otherwise wasted heat to convert into useful heat that can be used in multiple ways such as generating electricity [1, 2]. PV-T panels achieve this by several methods: the hybrid system can be designed with a flat plate collector in series with a PV panel as Tiwari and Kumar have shown in their research [3]. They can be used to produce steam in order to power a steam turbine as the Center of Environment and Energy Research & Studies (CEERS) have proposed or used to generate hydrogen fuel [4]. There are multiple usages for the useful heat gain from this hybrid system, however, they all share the

* Corresponding author
E-mail address: arabbeiki@es.isfpnu.ac.ir (M. Arabbeiki), sepahanshimi@gmial.com (M. Bakhshi)

same trait to improve overall efficiency over the traditional PV panel system. Some of the discussed systems could achieve overall efficiencies above 60%.

PV-T solar panels were first developed in the 1970s. During this period of time, pioneering work by wolf helped lay some fundamentals of Photovoltaic-thermal panels into whether they should use air or water as a cooling medium for the PV-T panels [5]. PV-T panel research then went to focus on using flat plate collectors [6, 7]. Flat plate collectors being a series of tubes contained a black solar radiation absorption material which allows heat transfer between itself and the tubes.

In addition to the flat plate collectors, solar concentrators which are referred to as concentrator type PV-T systems were developed in the 1990s. Solar concentrators are tubular shaped housings that receive reflected radiation from a concave disk/plate that receives solar radiation. The concavity of the disk/plate allows the radiation reflected on to the concentrator to be concentrated at a specific area or point, thus allowing higher heating temperatures of the fluid/air within the concentrator would be possible. Research by Akbarzadeh and Wadowski showed the benefits of using a heat pipe based on coolant design within the concentrator as opposed to applying air [8].

As noted in the previous sentences, there are two main types of heat transfer mode in Photovoltaic-Thermal panels, these PV-T panels that use the fluid as their main heat transfer medium and those that use air. A PV-T review by Chow showed that for those PV-T panels that use flat plate collectors, using a liquid system gave an overall efficiency ranging from 45% to 70% [9, 10]. The benefits of PV-T solar panels are that the conversion of heat to useful work helps with the decrease in efficiency of PV panel alone; that is, PV panels lose efficiency when the temperature of the panel gets above 50°C [11]. Using water or air to flow between the PV panel itself and a glass enclosure allows for cooling of the PV panel, which in turn allow the cell to work at a nearly optimum efficiency.

PV-T panels are currently being researched by several institutions worldwide such as the Indian Institute of Technology at Delhi, North Dakota State University and the City University of Hong Kong. New and novel and approaches in PVT design in recent years achieve higher efficiency when compared to traditional PV panels. This was demonstrated by the current research of Tawari and Rahul where they combined a PV-T system with a solar still in order to produce a continuous flow of freshwater [12]. Used concentrating solar collectors coupled with an organic Rankin power cycle (ORC) for seawater desalination co-generation. Although not directly mentioned, their system set-up constituted a PV-T design for producing desalinated water. The overall PV-T design goal is ultimately the same, and that is an improved power to cost ratio of PV-T system to those of PV and Thermal system working separately or in unison. This then entails an increase in efficiency of a joint system as appose to two separate working systems in whatever variation they may be set-up. As such, PV-T systems are the subject of interest of the proposed research.

2. Material and Method

2.1. PV-T System Design Components

Seawater will enter through a PVC pipe at Standard Sea Level conditions (SSL) of 15.5°C and 101.4 kPa. The saltwater will move to a reservoir which will hold the seawater at the desired pressure as shown in Figure 1. The desired fill level in the saltwater reservoir is maintained by a float valve so the saltwater never passes into the water vapour flow path. The seawater remains at the ambient temperature of 15.5°C in the reservoir. The seawater then leaves the reservoir into the PV-T.

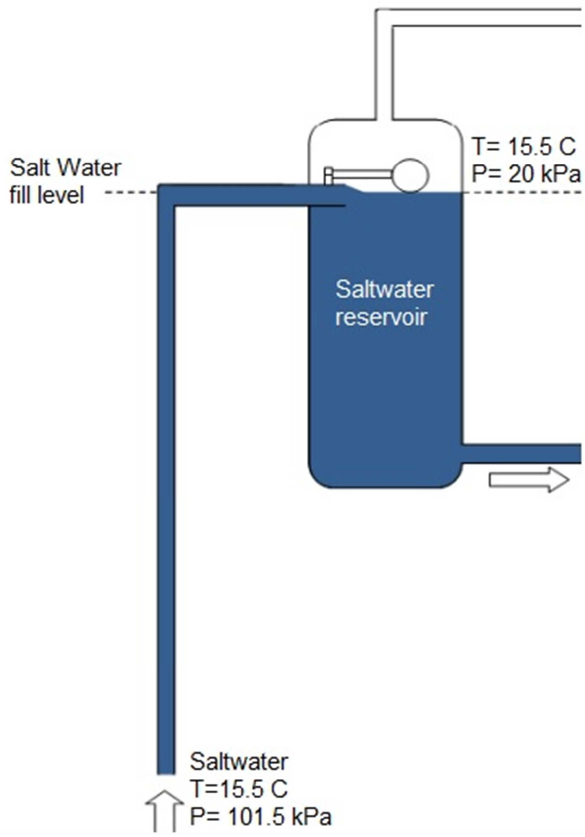

Figure 1. Saltwater reservoir filled at the desired level for desired pressure.

The use of a channel under the PV-T panel that uses silicone-based properties as shown Figure 2 and Figure 3, would house saltwater at all times. The photovoltaic cells will be facing the sun, while the shaded area underneath will form the top of the channel that is filled with seawater. The housing would be insulated as to minimize the heat loss to the environment. This will be either done by using exterior insulation encompassing the tank not facing the sun or the material of the tank would be self-insulating by the use of material with thick low emissivity properties. A float valve can control the level of water in the panel so that saltwater never passes into the water vapour flow path.

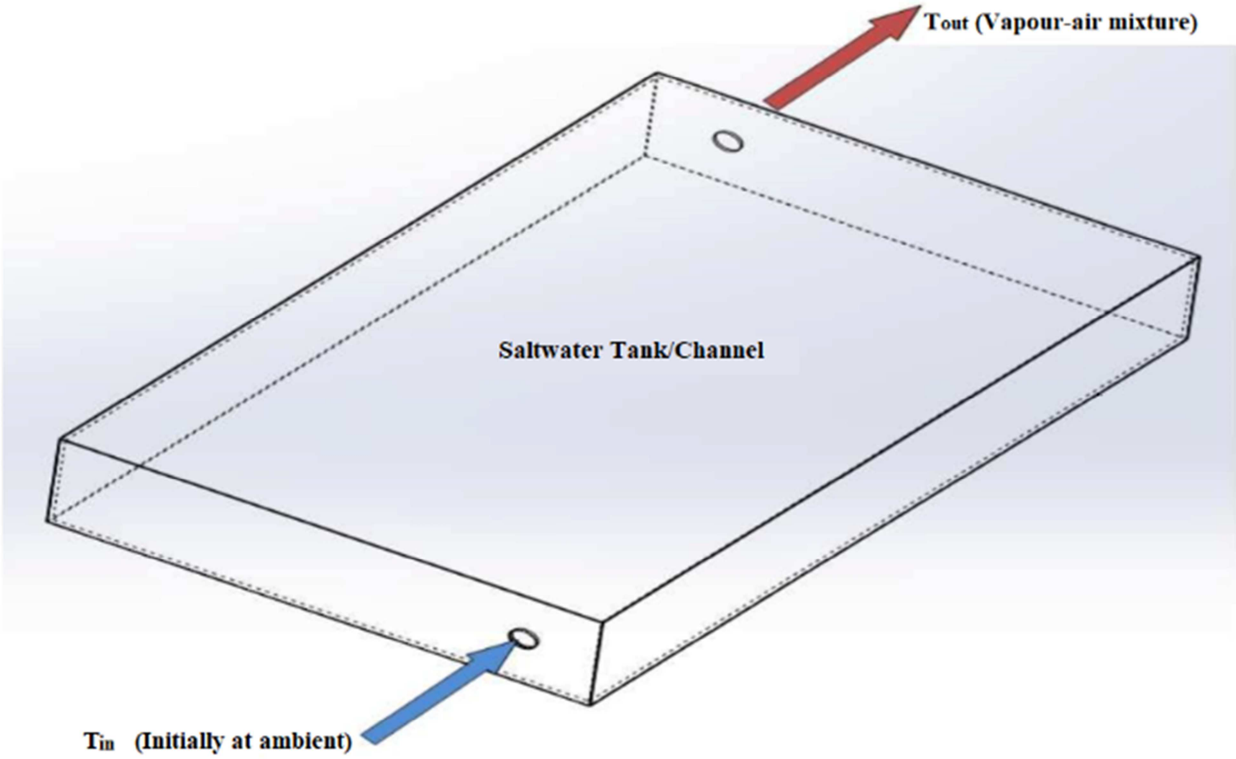

Figure 2. Isometric view of the PV-T housing used for saltwater desalination.

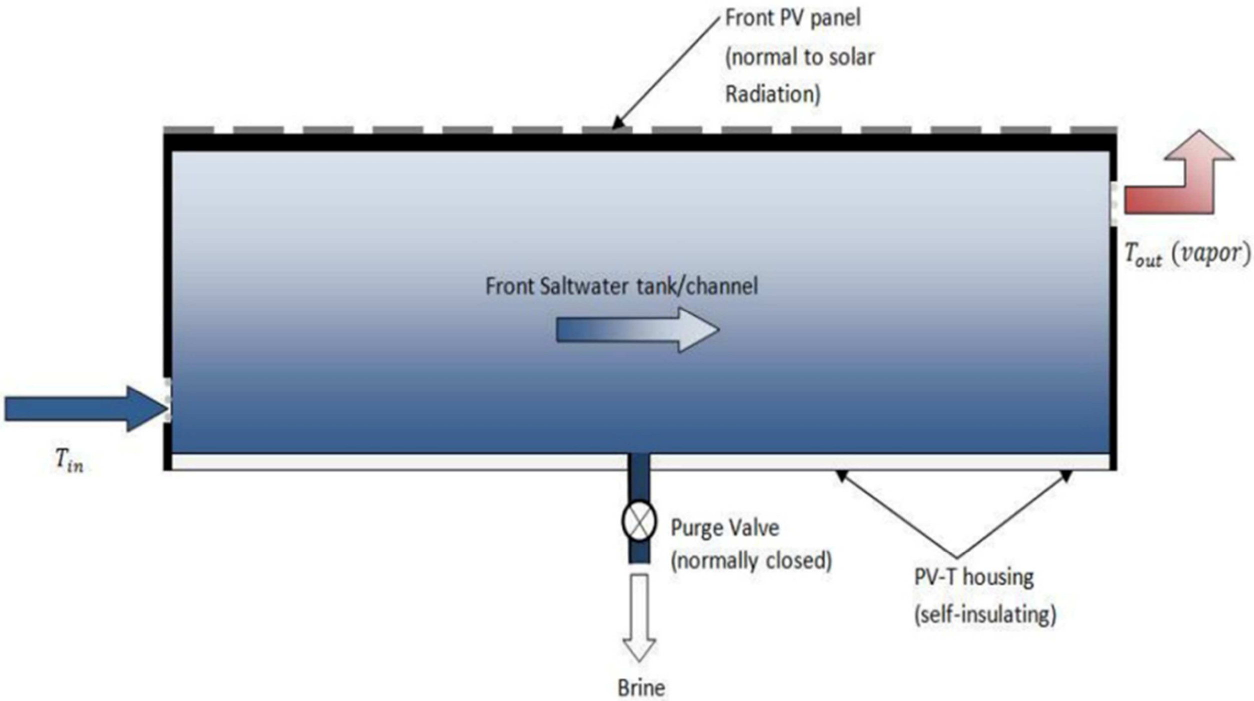

Figure 3. Front PV-T housing for saltwater desalination.

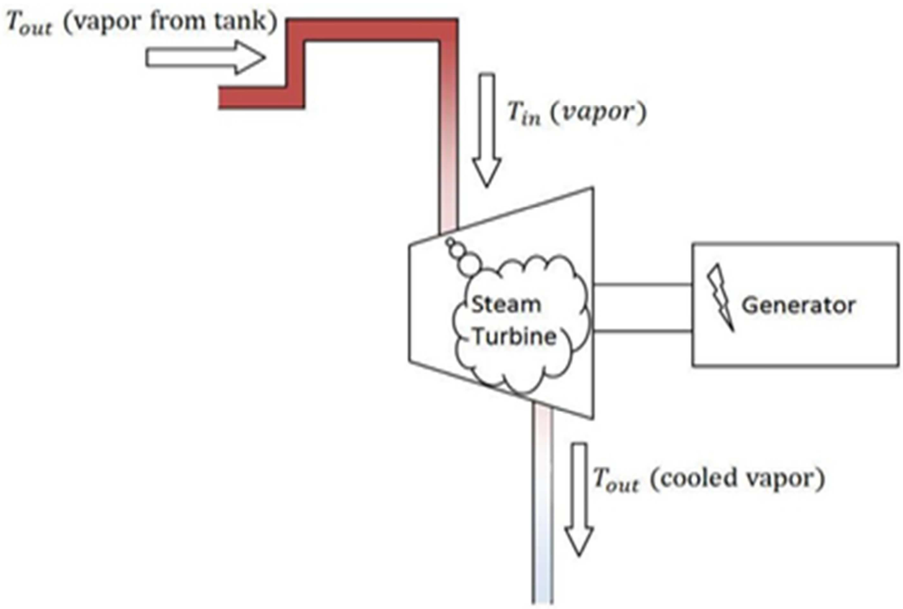

Figure 4. Vapour/steam going through a steam turbine to generate a current.

The condensing vapour-mixture then will be moved into a holding tank for further condenses as shown in Figure 5. Desorbed air percolates upwards inside the holding tank. The tank is large enough to hold the desorbed air and fresh water for a period of time until it is full and the need to relieve that tank would be necessary. Eventually, the desorbed air must be purged from the holding tank. This is done by a freshwater reserve tank that is located above the holding tank as shown in Figure 6. A purge valve opens allowing air to flow upward while fresh water flows downward. once the air is purged, the purge valve is closed and the system evacuates back down to the design pressure of 20 kPa by opening the valve to the gravity pump. Overall system is shown in Figure 4.

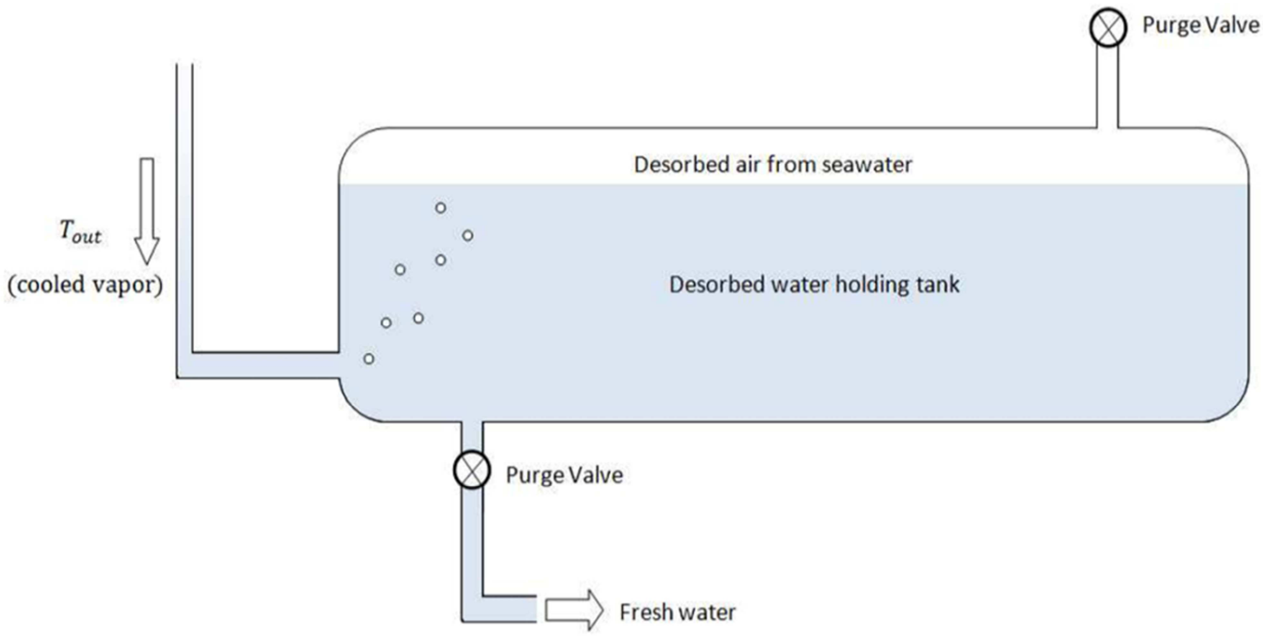

Figure 5. Desorbed water holding tank.

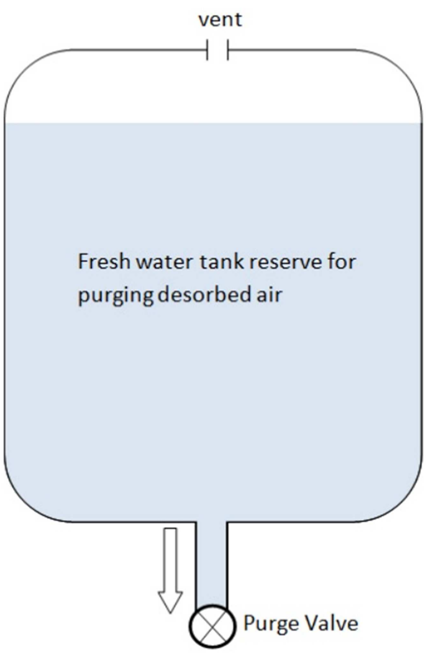

Figure 6. Fresh water holding tank for purging of desorbed air.

At a vapour pressure of 20 kPa, when the panel is heated to 60°C or greater, water vapour and desorbed gases from the seawater percolate upward and leave the housing where they travel a short distance through PVC (Polyvinyl Chloride) piping to the steam turbine. The air and vapour mixture passes through a steam-powered turbine and powers a generator, creating an electric current as shown in Figure 4. This is the main goal of the proposal whereas previously mentioned, a computational model will be used to show whether or not this PV-T design is feasible as there are multiple variables such as location, amount of incident solar radiation received by the PV panel, and so on, when working with such systems. Once work is done by the steam inside the turbine, the vapor mixture then leaves the turbine where it now has cooled down and begins to condensate.

2.2. Analytical Design Specifications

The research study will be composed of the above-mentioned components described in the previous section. However, when analytical calculations are performed, they will be limited to demonstrating the fundamentals. The fundamentals, which to minimize expenses in having to buy a high-cost PV panel, the absorptivity of the panel will be simulated by using a surface coated with black chrome on Ni-plated steel with Absorptivity, $\alpha = 0.95$ emissivity, $\varepsilon = 0.09$, thermal conductivity k, of 6.74 *Watt/cm. °C* as recommended by Mar and Zimmer [13]. Similarly, the steam turbine will be simulated, using an orifice to create that change in pressure and the subsequent drop in temperature. Lastly, the valves will be controlled manually and not with a controller [14].

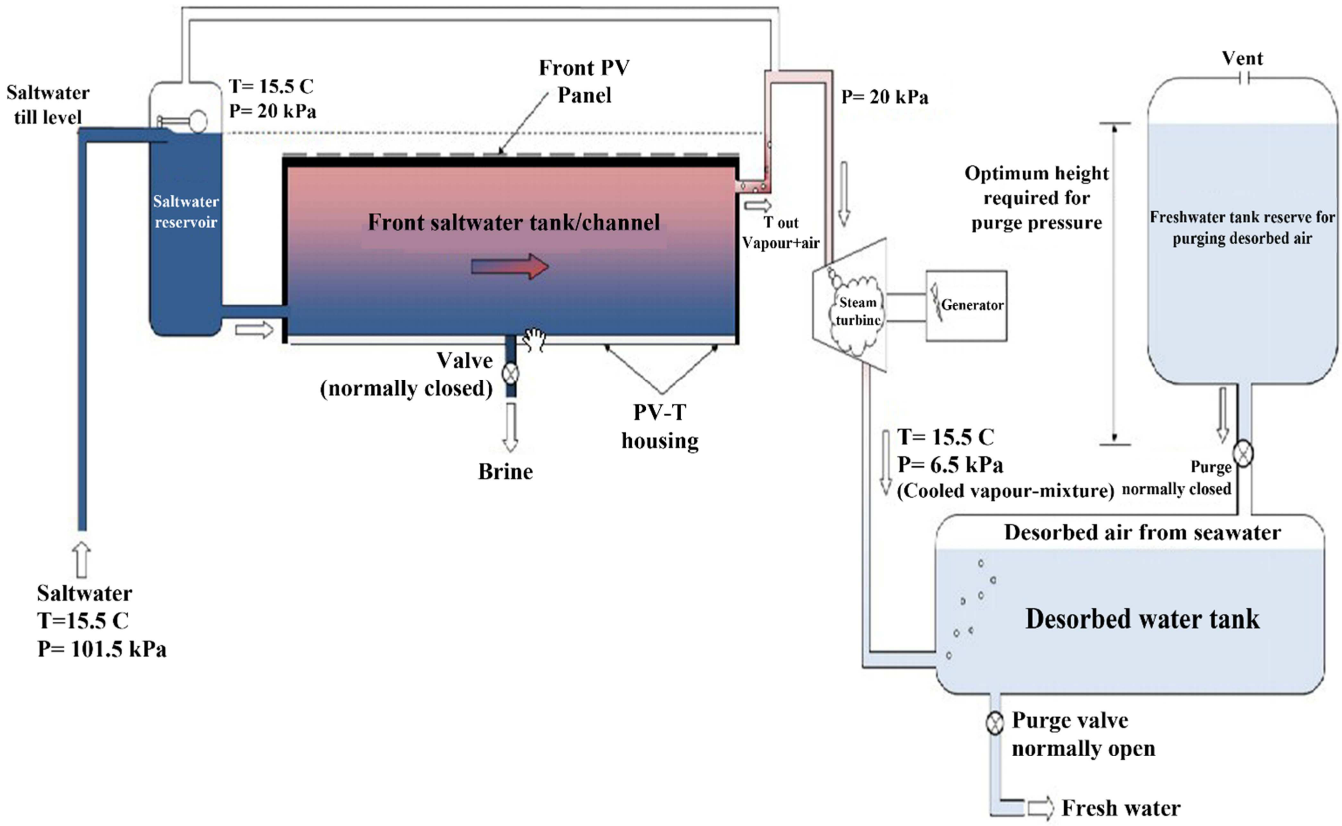

Figure 7. Solar power (PV-T) and desalination computer numerical model.

The PV-T performance required specifications remain the same whether using either PV-T or the black painted surface. These requirements along with the entire system for a computer numerical and the analytical demonstrator models assemblies are shown in Figure 7. Note that the models appear nearly identical with the exception that for the analytical model, the steam turbine-generator system has been replaced by an orifice and there is no PV panel on top of the saltwater housing. There is only now a black high absorptivity, low emissivity, painted surface.

2.3. PV-T Panel Equation Analysis

Analysis of solar radiation will be limited to those equation derived from previous analytical and experimental research in flat panel solar collectors [12, 15] and those of PV-T panels [16]. Similarly, the desalination process is analyzed using previous research by Tiwari and Rahul. The equations derived by Tiwari and Rahul are modified slightly to meet the design requirements of this study. Figure 8 shows the control volume for the PV-T design model, which is used in order to determine the conservation of energy, conservation of mass and more importantly for this design, useful heat gain by the saltwater in the tank-channel.

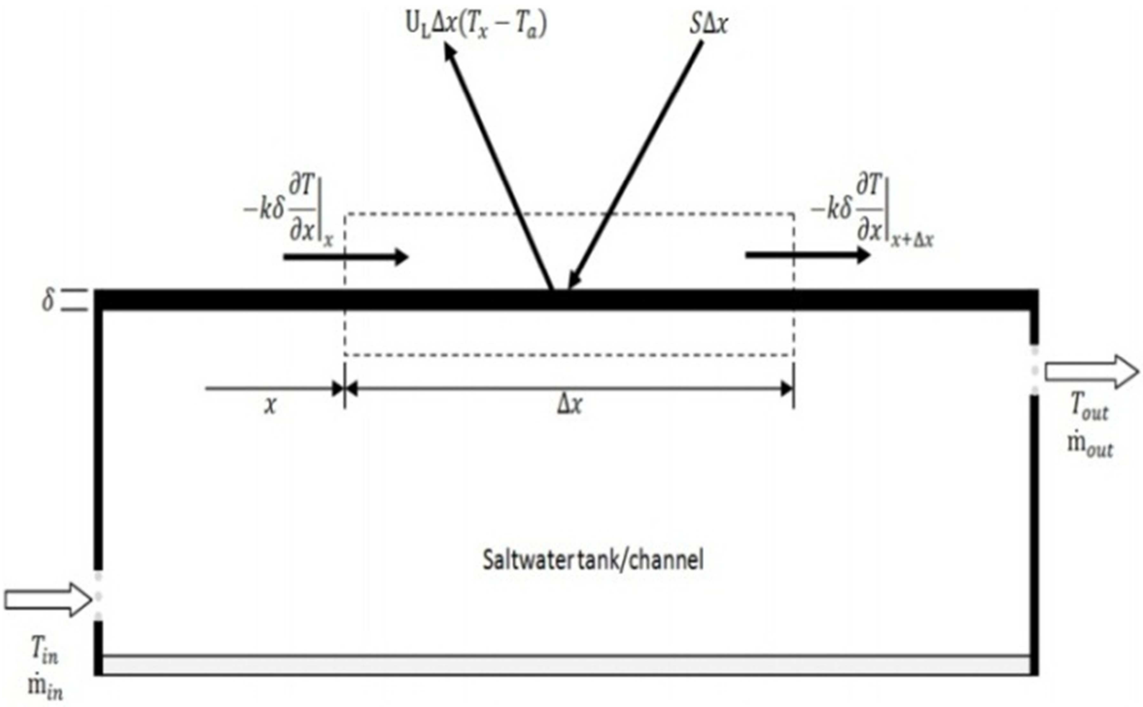

Figure 8. Control volume for the energy balance of the PV-T panel.

Thus, the conservation of energy for the incoming solar flux transfer to the black surface can be express as:

$$S\Delta x - U_L \Delta x (T - T_a) + \left(-k\delta \frac{\partial T}{\partial x}\right)|x - k\delta \frac{\partial T}{\partial x}|x + \Delta x = 0 \quad (1)$$

Where S is the absorbed solar energy, T_a is the ambient temperature of the surroundings, U_L is the total losses due to the material around the tank and emissivity, k is the thermal conductivity and δ is the thickness of the surface Dividing through by Δx and finding the limit as Δx approaches zero gives:

$$\frac{d^2T}{dx^2} = \frac{U_L}{k\delta}\left(T - T_a - \frac{S}{U_L}\right) \quad (2)$$

Eq (2) can be solved for the temperature distribution between the surface of the channel and the incoming solar radiation if the temperature gradient in the flow is temporarily negligible.

Using similarity transformations and applying boundary conditions on the symmetry at the centerline of the control volume, it is found that the temperature distribution becomes:

$$\frac{T - T_a - \frac{S}{U_L}}{T_b - T_a - \frac{S}{U_L}} = \frac{\cosh mx}{\cosh mW}, \text{ where } m = \sqrt{\frac{U_L}{k\delta}} \quad (3)$$

Here, T_b is the local base temperature on the surface of the saltwater PV-T tank-channel, and W is the width of the saltwater PV-T tank-channel surface that is normal to the incoming solar radiation. The useful heat gain by the black surface from the incoming radiation can then be expressed as:

$$\dot{q}_u = W\dot{F}[S - U_L(T_s - T_a)] \quad (4)$$

Where $T_{saltwater}$ is the local temperature of the saltwater inside the channel/tank, while F' is the collector efficiency and has been modified from that from Duffie and Beckman [15] to that of the PV-T tank-channel and is as follow:

$$F' = \frac{1}{\left(\frac{1}{F}+\frac{U_L}{\pi h_{s.i}}\right)} \quad (5)$$

Here, $h_{s,\ i}$ is the heat transfer coefficient between the saltwater and black surface. F is the black surface efficiency which relates losses through the material as:

$$F = \frac{\tanh(\frac{mW}{2})}{(mW/2)} \quad (6)$$

2.4. Saltwater Flow Equation Analysis

Eventually, the useful heat gain on the surface is transferred to the saltwater inside the channel/tank. The saltwater entering the channel initially enters at a specific temperature $T_{s,\ i}$, then the channel is heated and gain heat from the black surface to the desired temperature. The salt water then goes through desalination using an evaporative process and leaves the channel/tank at temperature $T_{s,o}$. Figure 9 shows the energy balance on the saltwater.

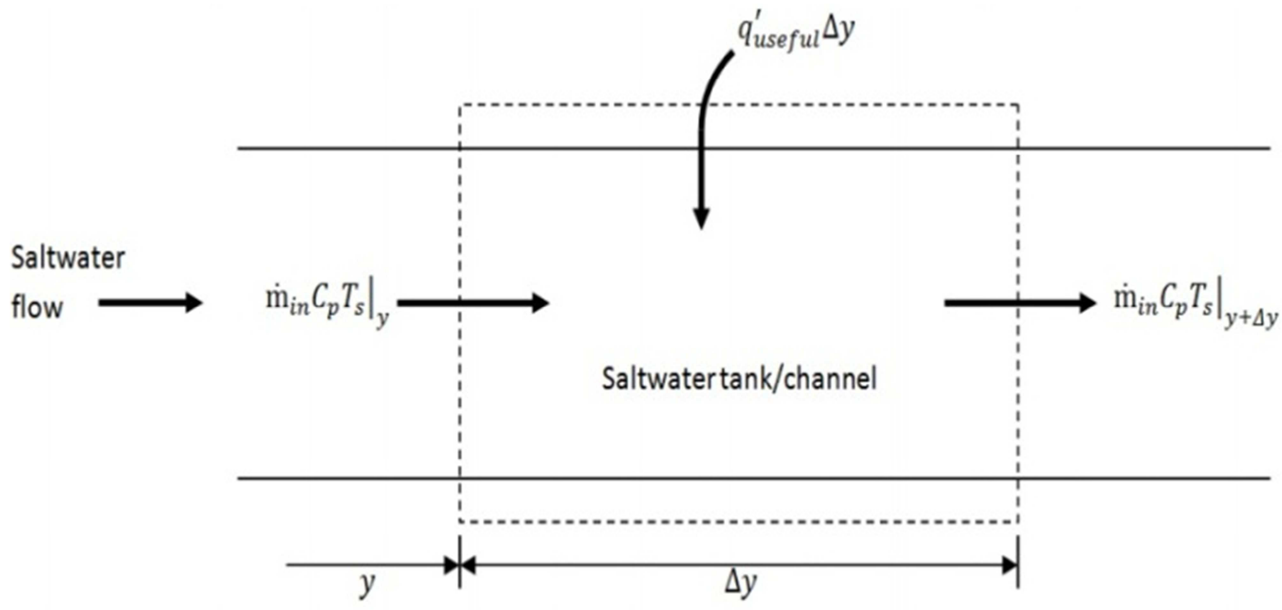

Figure 9. Control volume for the energy balance of the saltwater.

The energy balance of the saltwater flow is then:

$$\dot{m}C_pT_s|y - \dot{m}C_pT_s| + q'_u\Delta y = 0 \quad (7)$$

Where C_p is the pressure coefficient and $\dot{m}_{in}$ is the total flow rate. As before for the surface, dividing through by Δy and finding the limit as Δy goes to zero and substituting in for the useful gains q'_u, Eq (7) can be express as:

$$\dot{m}C_p\frac{dT_s}{dx} - WF'[S - U_L(T_{s.local} - T_a)] = 0 \quad (8)$$

Solving Eq (8) for temperature distribution of the saltwater flow with length L in the flow direction results in:

$$\frac{T - T_a - \frac{S}{U_L}}{T_b - T_a - \frac{S}{U_L}} = \exp\left(-\frac{U_LA_CF'}{\dot{m}C_p}\right) \quad (9)$$

Here, A_c is the tank-channel area and is equal to WL. Defining a quantity that relates the actual useful energy gain by the PV-T tank-channel to the useful gain, if the whole surface were at the saltwater inlet temperature is, this quantity is known as the collector heat removal factor F_R [12], The equation is:

$$F_R = \frac{\dot{m}}{A_C}\left(\frac{C_P(T_{s.i} - T_{s.i})}{S - U_L(T_{s.i} - T_a)}\right) \quad (10)$$

Using Eq (9), the above expression can be expressed as:

$$F_R = \frac{\dot{m}C_p}{A_CU_L}\left[1 - exp\left(-\frac{U_LA_CF'}{\dot{m}C_p}\right)\right] \quad (11)$$

F_R is tantamount to the effectiveness of a traditional heat exchanger; that is, the ratio of the actual heat transfers to the maximum possible. This maximum occurs at the inlet fluid temperature, thus heat losses to surroundings are at a minimum. The energy conducted to the region of the channel per unit length in the flow direction can now be found by evaluating Fourier's law and finding the actual useful energy gains Q_u:

$$Q_u = A_cF_R[S - U_L(T_{s.i} - T_a)] \quad (12)$$

The inlet temperature will be different than the ambient temperature due to the temperature gradient caused by the incident solar radiation. The local temperature must be found using an iteration approach. It is often more useful to use the mean fluid temperature using an iteration process to represent the inlet temperature. Akhtara and Mullickb showed that the mean fluid temperature to be [17]:

$$T_{f.mean} = T_{f.inlet} + \frac{Q_u/A_c}{F_R U_L}(1 - F'') \quad (13)$$

Where F'' is the collector flow factor defined as:

$$F'' = \frac{F_R}{F'} = \frac{\dot{m}C_p}{A_C U_L F'}\left[1 - exp\left(-\frac{A_C U_L F'}{\dot{m}C_p}\right)\right] \quad (14)$$

2.5. Determination of Tank Overall Heat Loss Coefficient U_L

For determining the overall heat loss coefficient of the PV-T tank-channel, there is a need to consider each boundary of each wall. This means the losses of both the top and bottom of the tank-channel housing and the losses of the edges/sides of the housing must be accounted for. For the losses on top of the PV-T tank-channel, U_{top}, an empirical equation developed by Buchovskaa [18], has acceptable results for mean plate temperatures between ambient and 200°C to within ±0.3W/m²°C. This equation is modified to fit the design requirements and is as follows:

$$U_{top} = \left(\frac{1}{h_w}\right)^{-1} \quad (15)$$

Here h_w is the wind heat transfer coefficient. This simplification is due to not having a glass cover over the black absorbing surface and is only dependent on the heat transfer coefficient of the saltwater with the surface. When calculating the losses at the bottom of the tank/housing, the loss is represented by the loss to the resistance in the insulation and the convection and radiation resistance to the environment. The bottom loss coefficient U_{bottom} can be approximated as:

$$U_{bottom} = \frac{k}{L} \quad (16)$$

Where L and k are the thickness and insulation thermal conductivity, respectively.

The edge loss is complicated to calculate due to the fact that at certain angles, absorption by the PV-T tank-channel will be occurring as solar radiations hit the edge surfaces. The edge losses are estimated by assuming one-dimensional sideways heat flow around the perimeter of the channel-tank housing. The losses through the edge should be compared to the channel-tank housing. The insulation is kept uniform throughout the sides and bottom of the channel-tank housing. Thus, accounting for the edge loss coefficient-area product $(U/A)_{edge}$ then the edge loss coefficient is:

$$U_{edge} = \frac{(U/A)_{edge}}{A_c} \quad (17)$$

The total loss coefficient can then be calculated as the sum of all loss coefficients, that is:

$$U_L = U_{top} + U_{bottom} + U_{edge} \quad (18)$$

Collector thermal performance comprises of three parts. Firstly, the instantaneous efficiency with directional radiation normal the black absorbing plate. Secondly, the effects of solid angle of incidence of the solar radiation, and lastly, the time constant for the channel-tank which is a measure of effective heat capacity must be found. The maximum useful heat gain is calculated by measuring the fluid inlet and outlet of the PV-T tank-channel, the incoming mass flow rate of the saltwater and the evaporation rate. The useful gain for the fluid is express as:

$$Q_u = \dot{m_{sw}} C_p (T_{s.o} - T_{s.i}) \quad (19)$$

To find the average evaporate rate, the following equation is utilized:

$$H_v = \frac{Q_u}{\dot{m}_{sw}} \quad (20)$$

Where H_v is found using the above two relationships and the fluid flow is found from empirical results for a specific geographic location. From this, data for both thermal output and on the conditions producing the thermal performance can be found and characterization of the PV-T panel can be determined by previous parameters. Eq (12) can be written in terms of the incident radiation as:

$$Q_u = A_c F_R\left[G_T(\tau\alpha)_{avg} - U_L(T_{s.i} - T_a)\right] \quad (21)$$

The local fluid temperature can be replaced by mean fluid temperature q, p without much loss in accuracy. The term $(\tau\alpha)_{avg}$ is the transmittance-absorptance product that is dependent on the beam, diffuse and ground radiations on the PV-T panel. This is expressed by Duffie and Beckman [15] as:

$$(\tau\alpha)_{avg} \cong 0.96(\tau\alpha)_b \quad (22)$$

$$(\tau\alpha)_b = 1.01\tau\alpha * {}^{a}/_{a_n} \quad (23)$$

Where the ratio of absorptance to that of absorptance

normal to incident radiation, a / a_n, is found based on the angle of incidence θ. The product (τα), for diffuse and ground radiations, can similarly be found using Eq 24. Here, the transmittance, τ is:

$$\tau = \frac{1}{2}\left(\frac{1-r_\parallel}{1+r_\parallel} - \frac{1-r_\perp}{1+r_\perp}\right) \quad (24)$$

Where $r_{/\!/}$ and $r\perp$ are the parallel and perpendicular components of the smooth surface when radiation passes through them. The relationships $r_\parallel$ and $r_\perp$ are referred to as Fresnel's Law of Refraction and are defined as:

$$r_{\parallel} = \frac{sin^2(\theta_2-\theta_1)}{sin^2(\theta_2+\theta_1)} \quad (25)$$

$$r_{\perp} = \frac{tan^2(\theta_2-\theta_1)}{tan^2(\theta_2+\theta_1)} \quad (26)$$

Here θ_1 and θ_2 are the angles of incidence and refraction, respectively. Using Analytical methods, the following equation can be used to find the angle of incidence:

$$\cos\theta = \sin\delta\sin\phi\cos - \sin\delta\cos\phi\sin\beta\cos + \cos\delta\cos\phi\cos\beta\cos\omega + \cos\delta\sin\phi\sin\beta\cos\gamma\cos\omega + \cos\delta\sin\beta\sin\gamma\sin\omega \quad (27)$$

Here ϕ is the latitude ω is the hour angle and γ is the surface azimuth angle; all which are prothe perty of the geographical location of the PV-T panel with respect to the sun. The declination δ can be approximated by an equation derived by Kabelac [19] as:

$$\delta = 23.45\sin\left(360 * \frac{284+n}{365}\right) \quad (28)$$

Here n is the numerical value of the date in a single year. The angle of refraction can be found using Snell's Law:

$$n_1\sin\theta_1 = n_2\sin\theta_2 \quad (29)$$

Where n_1 and n_2 are the refractive indices properties of the material. For the absorptance, the use of Kirchhoff's Law for radiation gives:

$$\alpha \cong 1-\tau \quad (30)$$

G_T in Eq (22) is the incident radiation and can be analytically calculated or found using empirical correlations. Using empirical correlations derived by Iqbal is expressed as [20]:

$$G_T = G_{on} = G_{sc}[1.000110 + 0.034221 Cos\ B + 0.001280\ sinB + 0.000719\cos 2B + 0.00077 sin2B] \quad (31)$$

Where G_{on} is the extra-terrestrial radiation incident on the plane normal to the radiation on a specific date and B is given by:

$$B = (n-1)\frac{360}{365} \quad (32)$$

Here n is once more the specific numerical date in a single year. G_{SC} is the solar constant. It is the energy from the sun per unit

time received on a unit area of a surface orthogonal to the direction of propagation of the radiation outside the atmosphere at some mean distance of the Earth to the Sun. G_{SC} has previously been calculated as:

$$G_{sc} = \begin{cases} 1367 W/m^2 \\ 433\ BTU/ft^2hr \\ 4.92 MJ/m^2hr \end{cases}$$

2.6. Efficiencies of PV-T Demonstrator

Now that the black surface useful gain and saltwater useful gain can be calculated, the instantaneous thermal and total saltwater efficiencies can be determined using the following equations:

$$\eta_{i.surface} = \frac{Qu}{A_cG_T} = F_R(\tau\alpha)_{avg} - \frac{F_RU_L(T_{s.i}-T_a)}{G_T} \quad (33)$$

And

$$\eta_{i.saltwater} = \frac{\dot{m}C_p(T_{s.o}-T_{s.i})}{A_cG_T} \quad (34)$$

The total efficiency of the tank-channel is the product of both the total useful heat the saltwater receives from the black surface and the useful heat the black surfaces receives from incident Radiation. As such, the total efficiency of the PV-T panel is then:

$$\eta_{i\ total} = \eta_{i\ surface} \times \eta_{i\ saltwater} \quad (35)$$

2.7. Analysis of the Desalination Process

The desalination process within the tank is governed by equations relating the salinity of the water, the minimum energy for desalination and vertical stratification phenomena known as a halocline. The design requirements dictate the PV-T tank-channel itself will have a height of one foot, halocline then has negligible effects and can be ignored A minimum amount of energy is required for salt and water to separate. This is known as Gibbs free energy. This process is irrespective of the actual evaporation that occurs due to heat addition to the saltwater. The minimal work required for the separation of water, and thus steam, from saltwater, is then the difference in the Gibbs energy:

$$w_{min} = \frac{m_{br}g_{br} + m_{v-a}g_{v-a} - m_{sw}g_{sw}}{m_{v-a}} \quad (36)$$

Here g is the specific Gibbs energy and is equal to $g=h-T*S$, h is the enthalpy, T is temperature and S in the entropy of the fluid [21]. The mass flow rate of the brim is the difference of the mass flow rate of water m_{sw} and that of the evaporation rate m_{v-a}. The minimum amount of work/energy must be achieved in order for desalination to happen before reaching a temperature where evaporation happens. From the preceding equations, it shows that minimum amount of energy for desalination must be found; otherwise, there is no possibility of steam production.

The amount of fresh water and thus steam that can be produced via desalination can be calculated using empirical data which found that for every 100 gallons of seawater that enters a desalination plant, 20 to 50 gallons exits as fresh water, the rest is flushed out as brine. With these empirical results, the actual efficiency range for a typical desalination plant is between 20% and 50% The analytical efficiency in desalination of the saltwater must also be taken into account as it is desired that effective desalination occurs at a rate where enough vapour-air mixture is produced in order to drive the steam turbine. A desalination efficiency correlation found by Gude is used in this study, which is [22]:

$$\eta_{desalination} = \frac{mh_{L(T)}}{\Sigma[Q_u(T_{s.o} - T_{s.i})]} \quad (37)$$

Where;

$$h_{L(T)} = 3.146 - 2.36(T + 273) \quad (38)$$

Here h is the latent heat of the saltwater at temperature T where desalination occurs, while Q_u is the useful heat gain found using Eq 20. A comparison of efficiencies can be made between the equations of instantaneous and desalination efficiency. It is be noted that the useful amount of heat absorbed by the saltwater Q_u, which also has to meet the minimum amount of work w_{min} for desalination to take place is the product of the total instantaneous efficiency and the desalination efficiency. Meaning, that the actual amount of desalination that occurs is expressed as:

$$\eta_{actual.pv-t} = \eta_{i.total} * \eta_{desalination} \quad (39)$$

2.8. Steam-Turbine Performance

As the analysis of PV-T tank-channel is largely complete, equations for the performance of the steam turbine are can be derived. A reasonable assumption where the loss in the PVC pipes, UKUH, is assumed to be minimal can be made due to a small length of travel in the PVC tubes. The energy balance for quasi-steady flow of the vapor-air mixture through the steam turbine is then:

$$\dot{E}in - \dot{E}out = \frac{dE_{system}}{dt} \quad (40)$$

Here $\dot{E}_{in}$ is the rate of net energy transfer in by heat, work, and mass, while $\dot{E}_{out}$ is the rate of net energy transfer out by heat, work and mass. Lastly, the expression on the right side of Eq 40 is the rate of change in internal, kinetic, potential and other energies. Taking a control area of the steam turbine, as shown in Figure 10, and after some time, assuming the flow to become steady-state, the above equation can be expressed as:

$$\dot{E}in - \dot{E}out = 0 \quad (41)$$

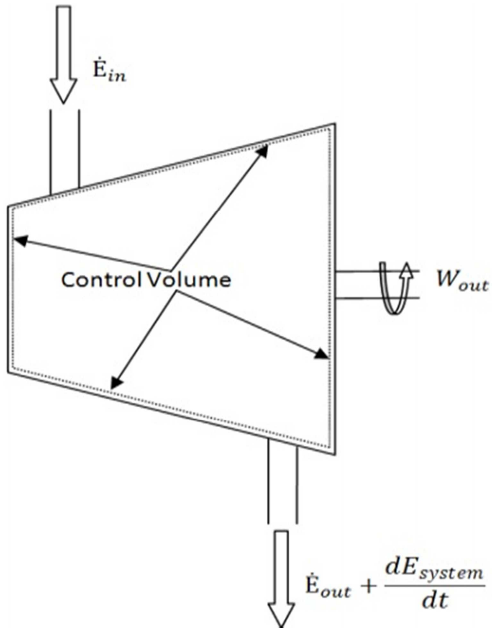

Figure 10. Control volume for the energy balance of the saltwater.

Taking into account that the incoming and outgoing energy is due to heat, work and mass, the energy balance in Eq 41 can be written as:

$$Q_{in} + W_{in} + \Sigma_{in} \dot{m}\left(h + \frac{V^2}{2} + gz\right) = Q_{out} + W_{out} + \Sigma_{in} \dot{m}\left(h + \frac{V^2}{2} + gz\right) \quad (42)$$

For this particular turbine, there is no heat addition to the system and no external work applied to it, the above relationship can then be written as:

$$(Q - W)\dot{m}\left[h_2 - h_1 + \frac{V_2^2 - V_1^2}{2} + g(z_2 - z_1)\right] \quad (43)$$

Here $q = Q/\dot{m}$ and $w = W/\dot{m}$. Given that the turbine is non-adiabatic and accounting for this value, Eq 43 can be expressed in terms of the work produced by the steam turbine. Thus:

$$w_{out} = h_1 - h_2 - \frac{V_2^2 - V_1^2}{2} + g(z_2 - z_1) - q_{out} \quad (44)$$

The mechanical efficiency of the turbine is taken to be $\mu_{mech} = 0.8$. The thermal efficiency of the system can be calculated by the following expression:

$$\eta_{th} = \frac{w_{out}}{q_{out}} \quad (45)$$

Thus, the total efficiency of the steam turbine is the product of the mechanical efficiency and that of the thermal efficiency. That is;

$$\eta_{total} = \frac{w_{out}}{q_{out}} \times \eta_{mech} \quad (46)$$

The actual amount of work is then found to be:

$$w_{actual} = \eta_{total} * w_{out} \quad (47)$$

2.9. Exergy Analysis of Steam Turbine

Since the steam turbine will also be working in an external environment, an exergy analysis of the steam turbine is required. For a fluid stream, exergy represents the greatest amount of useful work that is achieved as the system changes from one state to another in a particular environment. In an ideal case, this represents the reversible work w_{ref} in the system. As such, it is independent of the type of process, type of system, and the nature of energy interactions with its environment. Under these conditions, for the steam turbine in the study, the change in exergy, $\Delta\Psi$, as the vapour-air mixture travel from state 1 to state 2 is:

$$\Delta\psi = \psi_2 - \psi_1 = (h_1 - h_2) + T_a(s_2 - s_1) + \frac{V_2^2 - V_1^2}{2} + g(z_2 - z_1) \quad (48)$$

Here (s_2-s_1) is the change in entropy of the system that for this irreversible process, and is greater than zero. The entropy change of the system, when the vapour-air mixture is considered an ideal gas, can be found by:

$$s_2 - s_1 = \int_1^2 c_p(T)\frac{dT}{T} + Rln\frac{P_2}{P_1} \quad (49)$$

Where C_p is the specific heat, and R is the gas constant. For air at standard sea level conditions, the gas constant is equal to 0.286 kJ/kg°C.

2.10. Saltwater Reservoir Tank

Referring back to Figure 1, the saltwater Reservoir tank holds seawater with a salinity of 35 ppt (parts per trillion) and has an average density of 1027 kg/m³. The tank is filled to the desired level that is the same height as the PVC pipe leaving the tank-channel where evaporation occurs. This height is determined by the position of the reservoir tank with respect to that of the saltwater tank-channel housing. Determination of the volume of the tank-channel housing is first required before analyzing the volume requirements for the saltwater reservoir tank.

2.11. Tank-Channel Housing (PVT-Panel)

The area of the tank-channel housing is comparable to that of a basic photovoltaic panel. A typical 200-250 Watt PV panel normally has dimensions of 1.651 m for the length, 1.143 m for the width and 4.572 cm for the thickness, and weighs around 18.143- 22.67 kg. Given this, the area of concern is those that face directly the sun is 1.677 square meter. The PV-T tank-channel for this study will have a depth of 25.4 cm. This quantity can be optimized using analytical methods as it plays a pivotal role in not only how much useful energy is gained by the saltwater, but whether or not desalination and evaporation occurs.

Returning to the previous section regarding the saltwater reservoir tank, this tank can ideally be of any size as it will hold just saltwater. However, for analytical purposes, this tank will have a depth of 30.48 cm inches, with a length of 165.1 cm and a width of 101.6 cm.

The 101.6 cm represents the width of the tank-channel, while the depth is kept to 25.4 cm to ensure an equilibrium fill level and minimum heat loss of the vapour-air mixture leaving the PV-T tank-channel. Since the fill, level is to remain the same for the saltwater reservoir tank, and the flow is assumed laminar. The height the saltwater must travel to achieve a pressure difference of 81.35 kPa can be calculated by using the pressure difference between two points as:

$$h_{hs} = \frac{P_0 - P_1}{\gamma} \quad (50)$$

Here h_{hs} is called the pressure head, P_0 is the liquid pressure and γ is the specific weight of salt water which is equal to the product of the density of the fluid and gravity, $\gamma=\rho g$. The heat loss of the PVC going into the saltwater reservoir is of no concern as both the temperature at the PVC inlet and reservoir tank are at an ambient environmental temperature of T_a= 15.5°C.

The flow itself is assumed laminar in nature as the evaporation rate dictates the mass flow rate through the saltwater reservoir and subsequently, the PV-T tank-channel. The relationship between the pressures coming into the PVC pipe from a saltwater source, under the reasonable assumption that the density of the saltwater remains constant and incompressible under steady-state conditions at 101.5 kPa, to that of the saltwater reservoir 25.4 cm fill level of 20 kPa is related by Bernoulli's Equation as:

$$p_1 + \frac{1}{2}\rho V_1^2 + \gamma z_1 = p_2 + \frac{1}{2}\rho V_2^2 + \gamma z_2 + losses \quad (51)$$

Equation 37 is reduced to equation 36 under hydrostatic assumptions or when the flow is extremely slow, $v_{flow} \rightarrow 0$. Under similar assumptions, the mass flow rate ṁ can be found by continuity analysis and is related by what is known as the continuity equation in fluid mechanics, which suggest that mass is conserved throughout the system. For One Dimensional flow, this can be written as:

$$\dot{m}_1 = \rho_1 A_1 V_1 = \rho_2 A_2 V_2 = \dot{m}_2 \quad (52)$$

Here $A*V$ is the volumetric flow rate Ṽ. Returning the PV-T tank-channel, the saltwater mass flow rate entering the channel $\dot{m}_{in}$ is equal to the mass flow rates leaving as both as vapour-air mixture $\dot{m}_{out}$ and brime mixture $\dot{m}_{brime}$. Analytical, this conservation of mass can be expressed as:

$$\dot{m}_{sw} = \dot{m}_{v-a} + \dot{m}_{br} \tag{53}$$

2.12. Desorbed Water Holding Tank

The desorbed water holding tank is only as large as necessary. The purging of desorbed water is necessary at regular intervals in order to accommodate the flow rate of the condensing desorbed air from the saltwater. Referring back to Figure 5, the tank will hold 0.312 cubic meters of air store per 0.1 square meters of PV panel with a 10-minute purge cycle. Freshwater will leave the desorbed air tank at atmospheric pressure and at an estimated rate of 0.64 kg/hr.m². The tank will have to have a depth to meet these requirements and a combined length from the top purge valve to the PVC exit pipe of 81.3 cm of desalination liquid at 6.5 kPa. The purging process is achieved by the depth of the freshwater reserve tank. This process is explained in the following section.

2.13. Fresh Water Tank Reserve for Purging Desorbed Air

Referring back to Figure 6, the fresh water reserve tank will have depth as large as necessary to cause a purging of water in the desorbed water tank. This is achieved by finding the optimum column-depth height for the purge pressure, that is, it will use gravity to purge the desorbed water tank when the valve is open. As mentioned, this process is optimized and will be contingently based on the performance of the tank channel desalination process. The relationship uses to calculate the optimum height H, can be found by modification of Bernoulli's Eq (37) as:

$$H = z_2 - z_1 = \frac{V_2^2}{2g} + \frac{P_1 - P_2}{\gamma} + losses \tag{54}$$

If the losses due to friction within the PVC pipe are small enough that $\frac{P_1 - P_2}{\gamma} \gg losses$, then losses can be ignored. As such, the above equation can be written as:

$$H = z_2 - z_1 = \frac{V_2^2}{2g} + \frac{P_1 - P_2}{\gamma} \tag{55}$$

Here the subscripts 1 and 2 are arbitrary numbers used to refer to the top of the tank fill line and the purge valve interface, respectively.

2.14. Overall System Energy and Desalinated Water Production Efficiency

The Overall system efficiency can be determined from the dividing the sums of the actual heat gain by PV-T tank-channel housing and steam turbine actual output divided by the total intensity on such surface. Analytically, this can be shown as:

$$\eta_{overall.system\ energy} = \frac{W_{turbine\ out} + \sum Q_{actual}}{I_{total}} \tag{56}$$

The desalinated water production efficiency can be calculated by dividing the amount of distilled water produced by the amount of salt water coming into the system. Analytically, it is expressed as:

$$\eta_{distilled\ water\ production} = \frac{\dot{m}_{distilled}}{\dot{m}_{sw}} \tag{57}$$

Where

$$\dot{m}_{distilled} = \dot{m}_{v-a}$$

3. Result

3.1. Analytical Model Results

The results represent analytical outputs of the PV-T system under the following assumptions: Conditions are steady state, the flow is an elementary multi-phase and laminar, the environmental surroundings act as black body, individual phases have constant properties, losses due to friction in PVC pipes are negligible, top surface of PVT behaves as a gray smooth surface and is opaque to infrared radiation, position of PV-T panel is facing directly South from the Northern hemisphere, time of day is assumed to be on solar time, at a constant pressure in the PV-T tank-channel of 20 kPa, the saturation temperature is equal to 60°F at the PV-T panel outlet during steady state conditions, heat transfer through surfaces of PV-T panel considers one dimensional bi-directional, dust and dirt effects on top V-T surface are negligible, steam turbine is assumed adiabatic where losses are taking into account in thermal efficiency of the turbine, shading on PV-T is negligible, desorbed air at outlet behaves like an ideal gas.

3.2. PV-T (Tank Channel) Results

For the numerical year date of n=198 (July 17th 2015), during the period of 9:00 am to 6:00 pm, underachieved steady-state conditions, found using Eq (28), with the PV-T panel facing directly South towards the equator at a 30° slope, as detailed in Table 1, the results for the PV-T tank-channel under the aforementioned locality and given assumptions are expressed in the following subsections.

Table 1. PV-T System Performance Conditions (year date n=198).

Latitude	Declination	Slope	Orientation	Solar Time	Hour Angle
33°	21.2°	30˚	Due South	09:00hrs	-45°
33°	21.2°	30˚	Due South	10:00hrs	-30°
33°	21.2°	30˚	Due South	11:00hrs	-15°
33°	21.2°	30˚	Due South	12:00hrs	0°
33°	21.2°	30˚	Due South	13:00hrs	15°
33°	21.2°	30˚	Due South	14:00hrs	30°
33°	21.2°	30˚	Due South	15:00hrs	45°
33°	21.2°	30˚	Due South	16:00hrs	60°
33°	21.2°	30˚	Due South	17:00hrs	75°
33°	21.2°	30˚	Due South	18:00hrs	90°

Table 2. Desorbed Water Tank Analysis.

Tank height -Δz (m)	V_{exit} (m/s)	T_{out}, T_{exit} (°C)	P_{out}, P_{exit} (kPa)	$\dot{m}_{exit}$ (kg/hr.m²)
9.676	0.0468	17.8	101.4	12.329
9.676	0.0468	17.8	101.4	12.329
9.676	0.0468	17.8	101.4	12.329
9.676	0.0468	17.8	101.4	12.329
9.676	0.0468	17.8	101.4	12.329
9.676	0.0468	17.8	101.4	12.329
9.676	0.0468	17.8	101.4	12.329
9.676	0.0468	17.8	101.4	12.329
9.676	0.0468	17.8	101.4	12.329
9.676	0.0468	17.8	101.4	0

Table 3. Fresh Water Reserve Tank Analysis.

P_{top}(kPa)	V_{top}(m/s)-Initially static	V_{out}(m/s)-open valve	Specific heat-Fresh water (kJ/kg.c˚)	Specific weight of water (kg/m²s²)	Pbottom (kPa)	V_{out}(m/s)	Optimum height (m)
101.3	0	0.047	4.2	9797	131.2	0.047	3.05
101.3	0	0.047	4.2	9797	131.2	0.047	3.05
101.3	0	0.047	4.2	9797	131.2	0.047	3.05
101.3	0	0.047	4.2	9797	131.2	0.047	3.05
101.3	0	0.047	4.2	9797	131.2	0.047	3.05
101.3	0	0.047	4.2	9797	131.2	0.047	3.05
101.3	0	0.047	4.2	9797	131.2	0.047	3.05
101.3	0	0.047	4.2	9797	131.2	0.047	3.05
101.3	0	0.047	4.2	9797	131.2	0.047	3.05
101.3	0	0.047	4.2	9797	131.2	0.047	3.05

3.3. Desorbed Air and Fresh Water Reserve Tank Analysis

An analysis was performed on the desorbed water and fresh water reserve tanks to determine the optimum height for purging of the distilled water from the desorbed water tank, and calculating the amount of distilled water production in the process. Equations (36) through (40) were utilized to find the optimum height and mass flow rate. For the optimum height, an iterative process was implemented to find such value. Subsequent values where then found once the height was determined. These values are presented in Table 2 and Table 3.

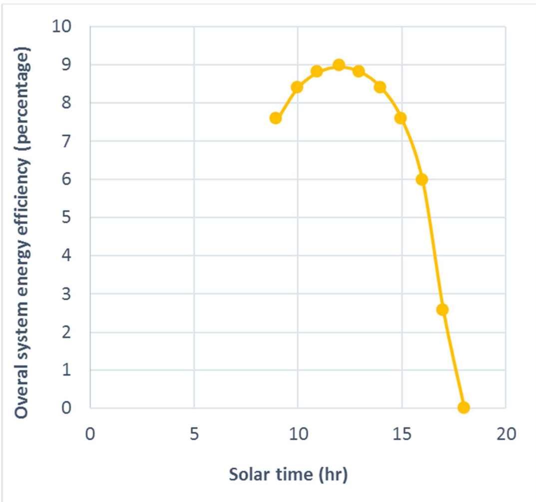

Figure 11. Overall system energy efficiency vs. solar time.

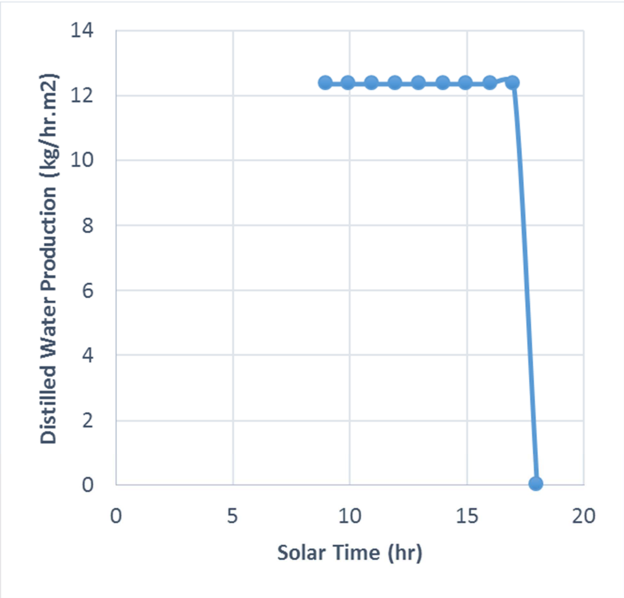

Figure 12. Distilled water production vs. solar time. Note: The values are considered constant as mass flow rate is kept constant until the end of the 10-hour period.

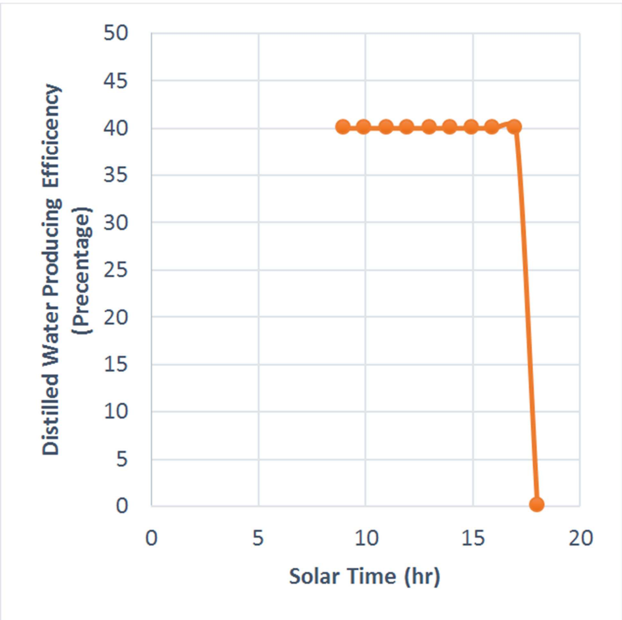

Figure 13. Distilled water production efficiency vs. solar time. Note: The values are considered constant as mass flow rate is kept constant until the end of the 10-hour period.

3.4. Overall PV-T System Performance

The overall PV-T system performance efficiency was determined using Eq (41), while the distilled water production amount is that of the already determined exit mass flow rate. The distilled water production efficiency was determined by using Eq (42). The following two pages show these values tabulated in Table 4 and plotted versus solar time in Figures 11 through 13.

Table 4. Overall PV-T System Performance Analysis.

Overall system energy efficiency (percentage)	Distilled water Production (kg/hr.m²)	Water production efficiency (percentage)
7.57	12.35254	39.96
8.4	12.35254	39.96
8.81	12.35254	39.96
8.94	12.35254	39.96
8.81	12.35254	39.96
8.4	12.35254	39.96
7.57	12.35254	39.96
5.94	12.35254	39.96
2.55	12.35254	39.96
0	0	0

4. Conclusion

Analysis of a PV-T system was performed that would intake saltwater or seawater as a working fluid, and pass it through a system that includes a Photovoltaic-Thermal panel, modelled as a tank channel with a black chrome surface, and produce drinkable water. Based on the surface properties, thermal radiation would heat up the saltwater/seawater to a point where there would be not only desalination but evaporation of vapour-air gas that would be used in a steam turbine to generate electrical power. The desorbed air would then condensate into desorbed distilled water that could be used for multiple purposes. The energy efficiency along with distilled water production rates of the system model was measured. An analytical system model was designed and results were tabulated. Optimization was performed on the analytical model in order to find the maximum yield of desalinated water production and power generated. Thereafter, the system energy efficiency and the desalinated water production efficiency were determined for the temperature distribution between the minimum saturation temperature and the maximum temperature. Results of the analytical analyses showed that at under the conditions and assumptions made, the average minimum efficiency of the system was around 7% for a 10-hour period. This is added to the efficiency of a traditional Photovoltaic panel, which would otherwise have wasted heat. This percentage, as previously noted, is the minimum energy produced by the steam turbine when the working fluid, i.e. saltwater for this study, reaches the evaporation temperature of T=60° C at a vapour pressure of P=20 kPa. Given that the aforementioned analysis is that of a noble approach, comparison to other studies is limited. One such study by Tiwari and Rahul had a solar still, which is a simple housing system for desalination which uses heat from the sun to drive evaporation from damp soil or saltwater reservoir, in series with two flat plate collectors. They used saltwater coming through the flat plate collectors to pre-heat the saltwater so once it reached the solar still, desalination would occur at a faster rate compared to not using the heat from the flat plate collectors.

Current maximum desalination yield of distilled water from seawater and brime is around 50%, with an average of 35%, the desalination process had an average production rate of 12.35 kg/(h.m²) and a water production efficiency of 40%, which is above the 35% average discussed in the Cooley study [23]. This value would vary under unsteady conditions. The water production rate and thus production efficiency would increase with an increase of outlet temperature as evaporation would occur at a faster rate.

Given this was a novel approach to desalination and power generation using a relatively new process of a tank-channel being fed by saltwater/seawater under a Photovoltaic panel which extracted the heat normally lost by the PV panel, there was no specific data available for comparison in this study. As such, the only true method of comparison is to perform an empirical study of this PV-T system set-up in order to determine the true feasibility of this model when compared to those results given by the analytical model. The production of desalinated water at a rate that is acceptable is of great interest to coastal geographical areas that may lack clean drinking water. This system model feasibly working can produce both desalinated drinkable water, and provide additional energy to power small electric appliances if installed at small scales of 1 or 2 units.

One recommendation of how to utilize this system would be to have an array of PV-T panel systems where the seawater would be pre-heated using tubes running in from the coastal seawater source prior to entering the panels in order to increased water production efficiency. This would require the utilization of a pump to move the saltwater from the source into the PV-T panel system. Another recommendation would be to have a system set-up next to existing power plants built near the coast, where the otherwise wasted heat could be utilized on the incoming saltwater to pre-heat the water before it enters the PV-T panel system. In either of these scenarios, the goal is to have enough PV-T panels to produce desalinated water in significant quantities that may remedy a clean water shortage.

References

[1] Singh, S., S. Agrawal, A. Tiwari, I. Al-Helal and D. Avasthi, Modeling and parameter optimization of hybrid single channel photovoltaic thermal module using genetic algorithms. Solar Energy, 2015. 113: p. 78-87.

[2] Dev, R. and G. Tiwari, Characteristic equation of a hybrid (PV-T) active solar still. Desalination, 2010. 254 (1-3): p. 126-137.

[3] Kumar, S. and A. Tiwari, Design, fabrication and performance of a hybrid photovoltaic/thermal (PV/T) active solar still. Energy Conversion and Management, 2010. 51 (6): p. 1219-1229.

[4] Licht, S., S. Ghosh, H. Tributsch and S. Fiechter, High efficiency solar energy water splitting to generate hydrogen fuel: Probing RuS2 enhancement of multiple band electrolysis. Solar energy materials and solar cells, 2002. 70 (4): p. 471-480.

[5] Wolf, M., Performance analyses of combined heating and photovoltaic power systems for residences. Energy Conversion, 1976. 16 (1-2): p. 79-90.

[6] Raghuraman, P., Analytical predictions of liquid and air photovoltaic/thermal, flat-plate collector performance. Journal of solar energy engineering, 1981. 103 (4): p. 291-298.

[7] Coventry, J. S., Performance of a concentrating photovoltaic/thermal solar collector. Solar Energy, 2005. 78 (2): p. 211-222.

[8] Akbarzadeh, A. and T. Wadowski, Heat pipe-based cooling systems for photovoltaic cells under concentrated solar radiation. Applied Thermal Engineering, 1996. 16 (1): p. 81-87.

[9] Li, C., Y. Goswami and E. Stefanakos, Solar assisted sea water desalination: A review. Renewable and Sustainable Energy Reviews, 2013. 19: p. 136-163.

[10] Chow, T. T., A review on photovoltaic/thermal hybrid solar technology. Applied energy, 2010. 87 (2): p. 365-379.

[11] Chen, X., L. Liu, Y. Y. Peter and S. S. Mao, Increasing solar absorption for photocatalysis with black hydrogenated titanium dioxide nanocrystals. Science, 2011. 331 (6018): p. 746-750.

[12] Li, C., G. Kosmadakis, D. Manolakos, E. Stefanakos, G. Papadakis and D. Goswami, Performance investigation of concentrating solar collectors coupled with a transcritical organic Rankine cycle for power and seawater desalination co-generation. Desalination, 2013. 318: p. 107-117.

[13] Mar, H. Y., R. Peterson and P. B. Zimmer, Low cost coatings for flat plate solar collectors. Thin Solid Films, 1976. 39: p. 95-103.

[14] Zefreh, M. A., Design and CFD Analysis of Airborne Wind Turbine for Boats and Ships. International Journal of Aerospace Sciences, 2016. 4 (1): p. 14-24.

[15] Duffie, J. A. and W. A. Beckman, Solar engineering of thermal processes. 2013: John Wiley & Sons.

[16] Bosanac, M., B. Sorensen, K. Ivan, H. Sorensen, N. Bruno and B. Jamal, Photovoltaic/thermal solar collectors and their potential in Denmark. Final Report, EFP Project, www. solenergi. dk/rapporter/pvtpotentialindenmark. pdf, 2003.

[17] Akhtar, N. and S. Mullick, Computation of glass-cover temperatures and top heat loss coefficient of flat-plate solar collectors with double glazing. Energy, 2007. 32 (7): p. 1067-1074.

[18] Buchovska, I., O. Liaskovskiy, T. Vlasenko, S. Beringov and F. M. Kiessling, Different nucleation approaches for production of high-performance multi-crystalline silicon ingots and solar cells. Solar Energy Materials and Solar Cells, 2017. 159: p. 128-135.

[19] Kabelac, S., Exergy of solar radiation. International journal of energy technology and policy, 2005. 3 (1-2): p. 115-122.

[20] Iqbal, M., An introduction to solar radiation. 2012: Elsevier.

[21] Çengel, Y. A. and M. A. Boles, Thermodynamics: An Engineering Approach, -PDF. 2008: McGraw-Hill.

[22] Gude, V. G., N. Nirmalakhandan and S. Deng, Desalination using solar energy: towards sustainability. Energy, 2011. 36 (1): p. 78-85.

[23] Cooley, H. and N. Ajami, Key issues for seawater desalination in California, in The World's Water. 2014, Springer. p. 93-121.